JOURNAL OF CATALYSIS **150,** 243–253 (1994)

The Inactivity of Extra Framework Aluminum in the Cracking of 2,3-Dimethylbutane on USHY

G. R. Bamwenda, Y. X. Zhao, and B. W. Wojciechowski[1]

Department of Chemical Engineering, Queen's University, Kingston, Ontario K7L 3N6, Canada

Received March 1, 1994; revised June 27, 1994

Activity and selectivity in the cracking of 2,3-dimethylbutane on steam-stabilized ultrastable HY (USHY), and on the same steamed USHY after extraction using $(NH_4)_2 SiF_6$, have been studied at 400°C. Based on the data presented here, a detailed mechanism is proposed for the cracking of 2,3-dimethylbutane on the two catalysts. The mechanism accounts for the kinetics and the selectivity behaviour observed and shows that extra-framework aluminum (EFAl) does not participate in the cracking of 2,3-dimethylbutane under our experimental conditions. Kinetic parameters obtained from the fit of experimental conversion data, and the initial product selectivities, show that monomolecular and bimolecular reactions are active on both catalysts. These quantitative measures show that extraction of EFAl from the steamed catalyst results in a small increase in the total intitial rate of reaction. We take this to indicate that new sites are activated by the removal of the EFAl. At the same time, product species are more strongly adsorbed on the extracted catalyst. As a result, a small increase in the rate of catalyst decay was noted on the extracted catalyst. The increase in initial rate of conversion is therefore negated at longer times on stream by the increase in the rate of catalyst decay. Selectivity data show that bimolecular reactions involving carbenium ions and feed molecules are dominant on both catalysts. No significant change in product distribution was observed upon removal of the extraframework aluminum. We conclude that the extraction of the EFAl increases the number of available sites without changing their acidity distribution. Such behaviour would be expected if the role of the EFAl is one involving purely mechanical blocking of feed accessibility to a random selection of active sites.

INTRODUCTION

Zeolites play an important role in catalysis, in particular in petroleum refining, and although the use of zeolite Y in catalytic cracking is common in practice, many of the details of its function in cracking remain a mystery. In particular, pretreatment methods and their effects on catalyst behaviour are poorly understood. The many methods of catalyst pretreatment, such as steaming and calcining, restructure the crystalline framework of the zeolite, producing extraframework aluminum (EFAl) which sits on the surface and in the pores of the zeolite crystallites. While it is well established that framework dealumination takes place during steam stabilization, resulting in the formation of EFAl, it may also be that some amorphous silica–alumina is formed in the debris. The EFAl or the silica–alumina debris may then modify catalyst activity or selectivity. There is much interest in the individual and collective roles of framework aluminum (FAl) and the EFAl (1–15) in studies aimed at unravelling the effects of these constituents on cracking. It has been variously reported that the effect of EFAl on catalyst activity is positive (1–6), negative (8–13), or none at all (14).

The principal methods used for preparing steamed Y zeolites free of EFAl are acid leaching with HCl (5, 15, 16) and with HNO_3 (11, 17), and treatment with ammonium hexafluorisilicate $(NH_4)_2SiF_6$ (18). The fluorosilicate (AHF) method is attractive because it seems to produce a zeolite free of crystal defects. Moreover, the reaction is carried out in an aqueous solution under relatively mild conditions.

By comparing the behaviour of steamed and $(NH_4)_2 SiF_6$ dealuminated zeolites Pellet *et al.* (9) concluded that the amorphous debris formed by dealumination with steam has an adverse affect on the cracking selectivity of gas oil to gasoline. Beyerlein *et al.* (5), working with FAV catalysts, showed that clean-framework zeolites prepared by $(NH_4)_2 SiF_6$ treatment are low in activity for isobutane cracking. They expressed the opinion that the observed lower activity and selectivity exhibited by this clean-framework material imply that dislodged aluminum species entrained in the lattice during hydrothermal treatment play an important role in the performance of ultrastable catalysts. Chauvin *et al.* (19), on the other hand, report that fluorosilicate treatment of faujasite, offretite, and mazzite catalysts resulted in a slight increase of the activity for isooctane cracking at 400°C, although deactivation characteristics and product distributions were little changed. Creighton *et al.* (14), using steam stabilized and $(NH_4)_2 SiF_6$ dealuminated zeolites, found identical prod-

---

[1] To whom correspondence should be addressed.

0021-9517/94 $6.00

uct selectivities in both catalysts. Our own kinetics and selectivity data (Tables 2–5) from the reactions of 2,3-dimethylbutane on ultrastable HY (USHY) and USHY–AHF show that dealumination of USHY with $(NH_4)_2SiF_6$ improves the activity via both monomolecular and bimolecular reactions, but causes no significant change in the initial selectivities.

In this work we present results from our studies on the cracking activity and selectivity of 2,3-dimethylbutane on USHY and USHY treated with ammonium hexafluorosilicate (USHY–AHF).

EXPERIMENTAL

The feedstock, 2,3-dimethylbutane (99+%), was obtained from Phillips Petroleum Co. and used without further purification. USHY was prepared from NaY, obtained from BDH, by repeated exchange with 0.5 *M* NH_4NO_3 solution at ~20°C for 24 h. Between exchanges the catalyst was dried at 110°C for 24 h, then calcined in air at 500°C for 2 h. After ten such exchanges the catalyst was steamed at 300°C for 24 h in 100% steam at atmospheric pressure. The samples were pelletized, crushed, and sieved to obtain the 60–80 mesh material used in our runs.

Ultrastable HY free of extra framework aluminum (USHY–AHF) was prepared by extracting the EFAl formed by steaming, using $(NH_4)_2SiF_6$. To prepare this sample, six grams of USHY were placed in a flask containing 450 cm^3 of 0.8 *M* ammonium acetate, and 16 cm^3 of 0.5 *M* $(NH_4)_2SiF_6$ was added slowly to the suspension while stirring (final pH = 6.5). The mixture was stirred for 3 h further at 80°C. The catalyst was filtered and washed thoroughly (15 washes) with distilled water then dried overnight in an oven at 110°C. After this treatment, the catalyst was pelletized, crushed, and sized to 60–80 mesh.

Samples of both catalysts were kept in a water-saturated atmosphere for 6 h at room temperature before the NMR experiments (21). The ^{27}Al MAS-NMR spectroscopy was conducted on a Brucker Am-400 spectrometer at 104.26 MHz, with Doty solid state accessories. Experimental conditions were: $PW = 1.2\ \mu s$ ($\simeq\pi/6$ pulse); RD = 0.5 s; SW = 50 kHz; SI = 4 k data points. A total of 5000 scans was collected for each spectrum at a spinning rate of 10 kHz. All ^{29}Si MAS-NMR measurements were carried out on a Brucker CXP200 spectrometer at 39.7 MHz. A pulse of 3 μs and recycling time of 10 s were applied at a spinning rate of 3 kHz.

Bulk Si/Al ratio of both catalysts was determined by elemental analysis, while framework Si/Al ratio was determined by X-ray diffraction. X-ray diffraction measurements were performed on a STOE STADI Z/OL instrument using Cu$K\alpha$ monochromated radiation $\lambda(K\alpha) = 1.54056$. As_4O_6 was used as an internal standard.

The conversion of 2,3-dimethylbutane was carried out in an isothermal plug-flow glass reactor (60 × 1.6 cm I.D.). The catalyst was diluted with sand, which was of slightly larger mesh size in order to minimize thermal effects and to facilitate the separation of catalyst from the sand. The catalyst bed length was 11 cm. Prior to each experiment the catalyst was purged for 30 min with nitrogen, *in situ* and at reaction temperature. Next, 2,3-dimethylbutane was pumped through the reactor at an appropriate rate. At various times, catalyst-to-reactant ratios between 0.0048 and 0.028 were used. This ratio was varied by changing the amount of catalyst in the reactor while the weight of the feed was kept constant.

Time on stream (TOS) was varied from 1.5 to 16 min by changing the feed rate of the reactant while keeping the total weight of feed-delivered constant. During the reaction, the liquid products were collected in a glass receiver and in a cold finger cooled in dry ice. The gaseous products were trapped in a gas burette by the downward displacement of water. At the end of each run, the reactor was purged with nitrogen (~150 cm^3/min, 40 min) and the purge gases were collected in the gas burette.

After every run, the catalyst was regenerated by passing dry carbon-dioxide-free air through the reactor (~160 cm^3/min) at 500°C for 8 h. Regeneration gases were passed through a second reactor containing an oxidation catalyst to ensure complete combustion to carbon dioxide and water. All water produced was trapped in 3A molecular sieves, while carbon dioxide was trapped in Ascarite followed by 13X molecular sieves. The amount of coke produced during the reaction was calculated from the weight of water and carbon dioxide trapped during regeneration.

Gaseous products in the range of C_1–C_4 were analyzed by a Carle SX 1156 gas chromatograph which also analyzed for H_2. Liquid products were analyzed by a Varian 6000 gas chromatograph with a 60-m SE54 capillary column and a flame ionization detector. Products up to C_7 were eluted at 0°C followed by a temperature program of 5°C/min up to 300°C. The identification of the liquid products was performed using a Finnigan 1020 GC/MS.

RESULTS

Physical Properties of the Catalysts

The physical and chemical properties of our catalysts are presented in Table 1. Treatment of USHY with $(NH_4)_2SiF_6$ resulted in an increase in the bulk and framework Si/Al ratios, and a decrease in the unit cell constant and in the number of aluminum atoms per unit cell.

Figures 1a and 1b present the ^{27}Al MAS NMR spectra of USHY (Fig. 1a) and USHY–AHF (Fig. 1b). Peaks I, II, and III represent in turn the tetrahedral FAl, and the penta- and octahedrally coordinated EFAl. As shown in Fig. 1b, treatment with $(NH_4)_2SiF_6$ results in the disap-

TABLE 1

Properties of the Catalysts Used in the Cracking of 2,3-Dimethylbutane

	Catalyst	
	USHY	USHY-AHF
Na^{+a}	<240 ppm	<230 ppm
$a_0(A)^b$	24.462	24.435
Si/Al (bulk)[a]	2.31	4.3
Si/Al (framework)[b]	6.13	7.04
Al atoms/UC (framework)[c]	27	24

[a] Determined by elemental analysis.

[b] Determined by X-ray diffraction.

[c] Determined according to the equation $N_{Al} = 112.1\ (a_0 - 24.222)$ in Ref. (20), where a_0 is the unit cell constant.

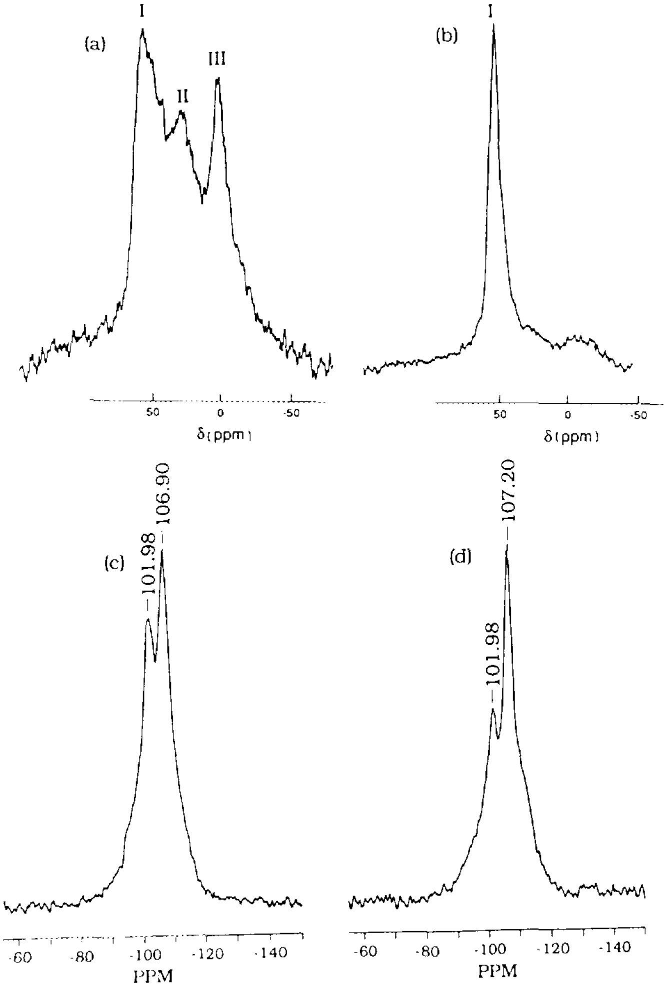

FIG. 1. ^{27}Al MAS NMR spectra of USHY (a) and USHY-AHF (b), and ^{29}Si MAS NMR spectra of USHY (c) and USHY-AHF (d) zeolites.

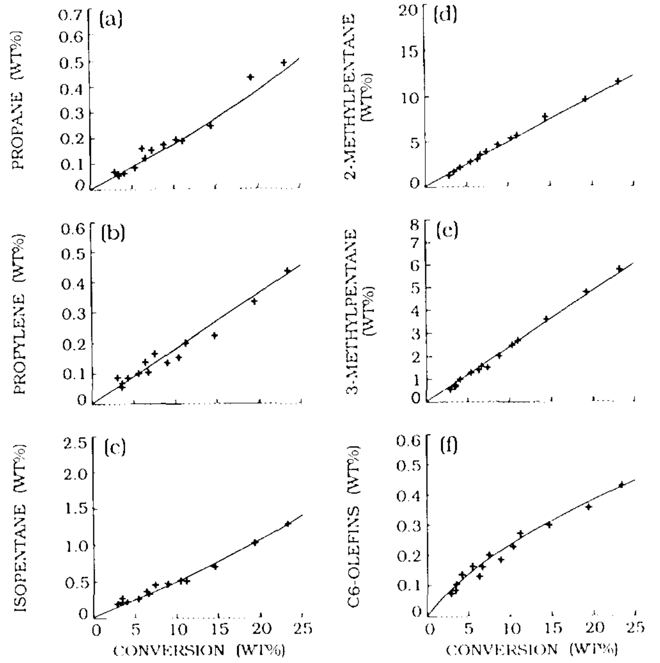

FIG. 2. Optimum performance envelopes for products of 2,3-dimethylbutane on USHY at 400°C: (a) propane, (b) propylene, (c) isopentane, (d) 2-methylpentane, (e) 3-methylpentane, and (f) C_6-olefins. Catalyst-to-reactant ratio: 0.0048–0.028.

pearance of the signals due to EFAl (peaks II, III), giving zeolite samples free of EFAl.

Figures 1c and 1d present ^{29}Si MAS NMR spectra of USHY (Fig. 1c) and USHY-AHF (Fig. 1d). Peaks at −101.98 and −106.90 ppm correspond to Si(1Al) and Si(0Al), respectively. After treatment with $(NH_4)_2SiF_6$ no new peaks appeared and there was no increase in the background in the vicinity of −107 ppm, indicating good retention of crystallinity. On the other hand, a decrease in the intensity of the signal due to Si(1Al) was observed, indicating the possible removal of some of the FAl.

Product Distribution and Selectivity

The products obtained during the catalytic cracking of 2,3-dimethylbutane on USHY and USHY-AHF include hydrogen, C_1, C_3–C_7 paraffins, C_2–C_8 olefins, C_7–C_{12} aromatics, and coke. Of these, only hydrogen, the C_1–C_6 compounds, and coke were found to be primary products. Figures 2 and 3 show some examples of product yields vs corresponding conversion on USHY and USHY-AHF catalysts, respectively. Initial selectivities and product types were obtained by drawing optimum performance envelopes for the products and determining selectivity behaviour at zero conversion. Product types and initial weight and molar selectivities for primary products for both catalysts are listed in Table 2.

As can be seen in Table 2, the product distribution

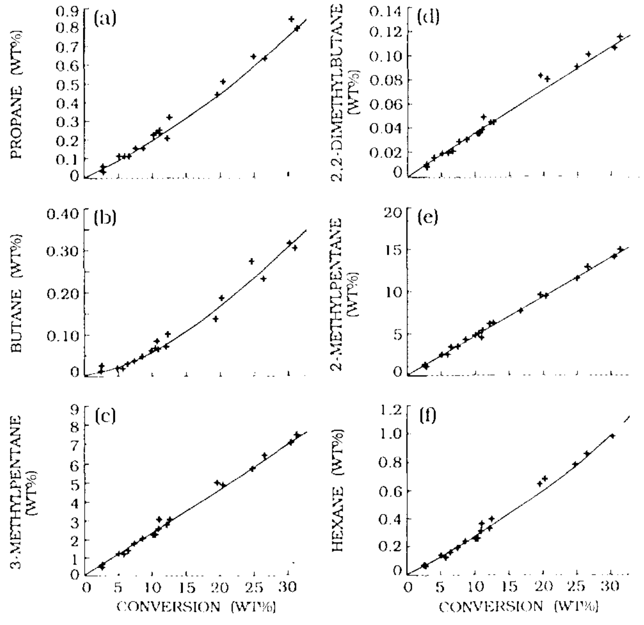

FIG. 3. Optimum performance envelopes for products of 2,3-dimethylbutane on USHY–AHF at 400°C: (a) propane, (b) butane, (c) 3-methylpentane, (d) 2,2-dimethylbutane, (e) 2-methylpentane, and (f) hexane. Catalyst-to-reactant ratio: 0.0051–0.026.

obtained from 2,3-dimethylbutane cracking is quite similar on both catalysts. On both catalysts, the primary products consisted mostly of 2,3-dimethylbutane skeletal isomers, i.e., 2-methylpentane, 3-methylpentane, 2,2-dimethylbutane, and *n*-hexane, which together make up about 80% of all initial products. Other significant primary products include hydrogen, methane, propylene, C_3–C_5 paraffins, and C_6 olefins. It is worth noting that ethane was not detected in the products. All this seems reasonable since ethane and C_4 olefins cannot be produced by the direct scission of any one bond in 2,3-dimethylbutane. Ethylene, C_4 olefins, and C_4 paraffins are products one may expect from β-cracking of surface resident isomeric species and from various disproportionation reactions, as will be discussed below. The detection of 2,2 dimethylbutane as a primary product was surprising, in view of long-standing theories concerning the reactions of carbenium ions which reject the possibility of the formation of quaternary carbon species.

In addition to primary products, the reaction output contained various secondary products, which altogether constitute less than 7% of all products under most conditions. Figure 4 presents some examples of secondary product yields vs conversion on USHY (Figs. 4a–4d) and USHY–AHF (Figs. 4e–4h). As was the case with primary products, the yield and distribution of secondary products was very similar on both catalysts. Secondary products consist largely of methylcyclopentane, C_7-paraffins and olefins, C_8-olefins, and C_7-C_9 aromatics. Aromatics with carbon numbers higher than 9 were relatively minor products and consisted of tetramethylbenzenes, dimethyldiethylbenzenes, and alkylated naphthalenes.

DISCUSSION

Reaction Mechanism

It is widely accepted that the conversion of paraffins over solid acid catalysts proceeds via carbocation intermediates, i.e., carbonium and carbenium ions (22, 25). Recent studies of 2-methylpentane cracking on USHY (22) as well as dilution studies using nitrogen (23) have indicated that the cracking of that branched C_6 paraffin follows both monomolecular and bimolecular modes of reactions. From the product distributions presented in Tables 2 and 3 it is evident that 2,3-dimethylbutane reactions also cannot be explained as resulting from monomolecular processes alone. To explain the observed product distributions and selectivities we propose the following reaction scheme for 2,3-dimethylbutane cracking at 400°C over USHY and USHY–AHF.

(*i*) *Monomolecular cracking.* Initiation of the reaction sequence occurs by the protonation of the 2,3-dimethylbutane molecule at a Brønsted acid site, forming a carbonium ion (22). The formation of hydrogen can then be accounted for by the protolytic cleavage of a C–H bond, releasing molecular hydrogen and leaving a parent carbenium ion on the Brønsted site

$$C_6H_{14} + H^+B^- \rightleftarrows C_6H_{15}^+B^- \rightarrow H_2 + C_6H_{13}^+B^-, \qquad [1]$$

where $C_6H_{15}^+$ and $C_6H_{13}^+$ denote carbonium and carbenium ions, respectively.

The formation of the light paraffins C_1 and C_3 can be accounted for by the protolytic cleavage of a C–C bond of the parent carbonium ion. This will produce an alkane C_iH_{2i+2} and a carbenium ion $C_jH_{2j+1}^+$ with $i + j = 6$, according to the general equation

$$C_6H_{14} + H^+B^- \rightleftarrows C_6H_{15}^+B^- \rightarrow C_iH_{2i+2} + C_jH_{2j+1}^+B^-, \qquad [2]$$

where $i = 1$ or 3 in this case.

The larger of the carbenium ions from reactions 1 and 2 can undergo skeletal isomerization, i.e., methyl and hydride rearrangements, according to

$$C_jH_{2j+1}^+B^- \rightleftarrows \text{iso-}C_jH_{2j+1}^+B^-, \qquad [3]$$

where iso-$C_jH_{2j+1}^+$ is the isomerized carbenium ion. At any instant any such carbenium ion can desorb as an olefin C_jH_{2j} according to

TABLE 2

Initial Selectivities for Cracking Reactions of 2,3-Dimethylbutane over USHY and USHY–AHF at 400°C

			Initial selectivity			
	Type[a]		Weight[b]		Molar[c]	
Products	USHY	USHY–AHF	USHY	USHY–AHF	USHY	USHY–AHF
Hydrogen	(1 + 2)S	(1 + 2)S	0.0007	0.0008	0.0301	0.0344
Methane	1S	1S	0.0040	0.0037	0.0215	0.0199
Ethane	—	—	—	—	—	—
Ethylene	1S	1S	0.0021	0.0015	0.0065	0.0046
Propane	(1 + 2)S	(1 + 2)S	0.0184	0.0203	0.0360	0.0397
Propylene	1S	1S	0.0194	0.0206	0.0397	0.0422
Isobutane	(1 + 2)S	(1 + 2)S	0.0250	0.0330	0.0371	0.0489
n-Butane	(1 + 2)S	(1 + 2)S	0.0038	0.0041	0.0056	0.0061
C_4-Olefins	(1 + 2)S	(1 + 2)S	0.0026	0.0030	0.0040	0.0046
Isopentane	(1 + 2)S	(2 + 2)S	0.0525	0.0510	0.0627	0.0609
n-Pentane	(1 + 2)S	(1 + 2)S	0.0021	0.0026	0.0025	0.0031
C_5-Olefins	1S	1S	0.0084	0.0091	0.0103	0.0112
2,2-Dimethylbutane	1S	1S	0.0038	0.0038	0.0038	0.0038
2-Methylpentane	1S	1S	0.5359	0.5261	0.5359	0.5261
3-Methylpentane	1S	1S	0.2531	0.2509	0.2531	0.2509
n-Hexane	1S	1S	0.0282	0.0293	0.0282	0.0293
C_6-Olefins	1U	1U	0.0323	0.0317	0.0331	0.0325
Coke	(1 + 2)S	(1 + 2)S	0.0054	0.0064	0.0054	0.0065
Total			0.9977	0.9980	1.1154	1.1247

[a] Determined according to the slope of OPE curve at origin, i.e., nonzero for primary and zero for secondary (24).

[b] Obtained from the slope of OPE curve at origin (24).

[c] Calculated using the relationship:

$$\text{Molar selectivity} = \text{weight selectivity} \cdot \frac{\text{molecular wt. of feed}}{\text{molecular wt. of product}}.$$

$$C_jH^+_{2j+1}B^- \rightleftarrows C_jH_{2j} + H^+B^-. \qquad [4]$$

The lifetime of the carbenium ions on the surface depends on the strength of the acid sites on the catalyst surface, on the reaction temperature, and on the presence of reactants which may encourage desorption. One can expect that the lifetime of a carbenium ion is longer at low reaction temperatures (22) and on catalyst surfaces with strong acidic sites (12).

(*ii*) *Bimolecular reactions.* Examining the results presented in Table 2, it can be seen that, for example, the molar ratio methane/C_5-olefins is greater than unity. A value of unity would be expected if the source of these species were exclusively monomolecular protolysis of 2,3-dimethylbutane. The disparity indicates that some of these products are generated not only by the above monomolecular reaction but also by other processes. This fact, as well as the production of primary ethylene, C_4 olefins and paraffins, and C_5 paraffins shown in Table 2, leads us to suggest that in addition to monomolecular processes, cracking of 2,3-dimethylbutane over USHY and USHY–AHF proceeds via bimolecular processes.

(a) Hydride abstraction. The carbenium ion formed in reactions [1] and [2] can carry on chain propagation reactions by acting as a Lewis acid and abstracting a hydride ion from a feed molecule. This leads to a product paraffin and a new (parent) ion (Eq. [5]) which can further propagate the hydride transfer chain reaction:

$$C_jH^+_{2j+1}B^- + C_6H_{14} \rightarrow C_jH_{2j+2} + C_6H^+_{13}B^-. \qquad [5]$$

Hydride abstraction by $C_6H^+_{13}B^-$ species, which have undergone a number of methyl and hydride shifts, leads to the formation of isomeric C_6 paraffin products:

$$\text{iso-}C_6H^+_{13}B^- + C_6H_{14} \rightarrow \text{iso-}C_6H_{14} + C_6H^+_{13}B^-. \qquad [6]$$

The ease with which the chain processes occur depends on the rate of hydride abstraction from the donating molecule. 2,3-dimethylbutane, with two tertiary hydrogen atoms, can donate a hydride quite readily and therefore vigorously promotes chain reactions. Since 2,3-dimethylbutane skeletal isomers constitute about 80% of all the

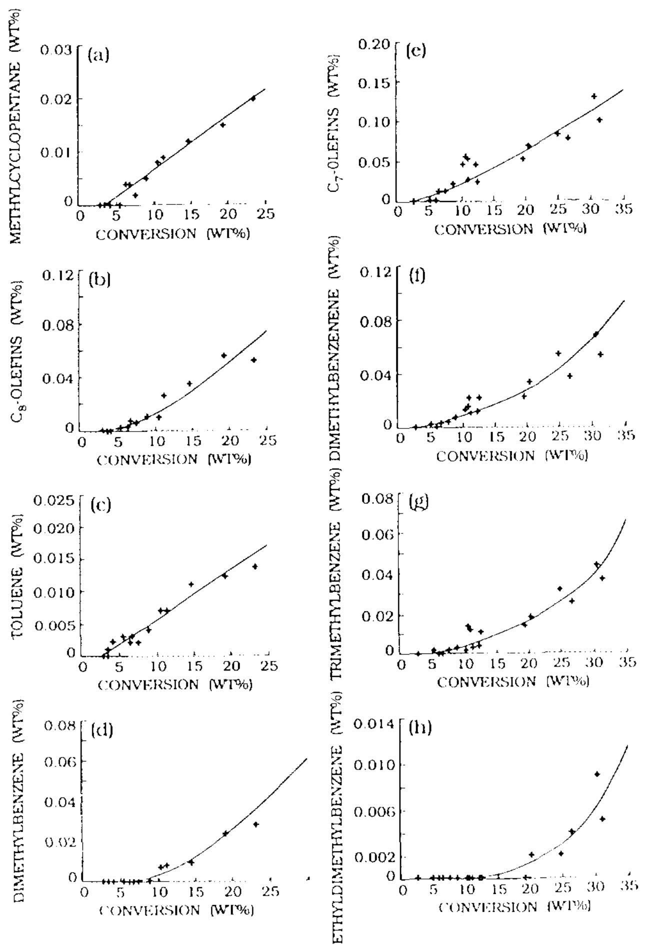

FIG. 4. Yield of secondary products vs conversion of 2,3-dimethylbutane on USHY (a–d) and on USHY-AHF (e–f) at 400°C: (a) methylcyclopentane, (b) C_8-olefins, (c) toluene, (d) dimethylbenzenes, (e) C_7-olefins, (f) dimethylbenzenes, (g) trimethylbenzenes, and (h) ethyldimethylbenzenes. Catalyst-to-reactant ratios are as in Figs. 2 and 3.

initial products we can conclude that the process shown in Eq. [5] is the dominant reaction mode in the cracking of 2,3-dimethylbutane at 400°C on both USHY and USHY-AHF. The termination step always involves back donation of a proton to the Brønsted base by an adsorbed carbenium ion and the consequent desorption as an olefin:

$$C_iH_{2i+1}^+B^- \rightleftarrows C_iH_{2i} + H^+B^-. \qquad [7]$$

TABLE 3

Optimum Values for Kinetic Parameters for Cracking of 2,3-Dimethylbutane on USHY and USHY-AHF at 400°C (N fixed at 1.0)

Kinetic Parameters	USHY	USHY-AHF
A_1(min^{-1})	0.564	0.505
A_2(min^{-1})	−0.0619	−0.0809
B	−0.807	−0.912
G(min^{-1})	0.103	0.123
N	1.0	1.0
$\Sigma \mathcal{F}_i$	1.1154	1.1247
C_{A_0}(mol dm^{-3})	0.018	0.018

(b) Disproportionation. A carbenium ion formed from reactions [1]–[3] can also act as a Brønsted acid and protonate a feed molecule to form an oligomeric carbonium ion. This can subsequently either desorb or undergo decomposition into an alkane and a new carbenium ion:

$$C_jH_{2j+1}^+B^- + C_6H_{14} \rightleftarrows C_{(6+j)}H_{2(6+j)+3}^+B^- \rightarrow$$
$$C_nH_{2n+2} + C_{6+j-n}H_{2(6+j-n)+1}^+B^-. \qquad [8]$$

The fact that C_7–C_{11} species were not observed as primary products indicates that in our system, carbonium ions of that size fragment into smaller products before desorption. Such oligomeric products may well form from carbonium ions on other catalysts, or at lower temperatures, and they do form here at higher conversion but by a different path. At higher conversion they form from carbenium ions which arise when product olefins add to surface carbenium ions, thus forming larger oligomeric carbenium ions. As a result, these larger products appear in our secondary products only.

Equations [4] and [7] account for the formation of ethylene and C_4 olefins, while Eqs. [2], [5], and [8] illustrate the formation of various paraffins such as C_5 and C_6. Among these there are various C_6 paraffins formed by the transfer of a C_1 group to a C_5 ion by a process illustrated in Eq. [8]. Among those in turn, some of the transfers of a C_1 group will have taken place to tertiary C_5 ions. It is those select few reactions which quite straightforwardly yield the unexpected product 2,2-dimethylbutane.

The proposal that 2,2-dimethylbutane is not formed by the direct isomerization of a hexyl carbenium ion is supported by the absence of 2,2-dimethylbutyl olefins in the products. If hexyl carbenium ions could rearrange to form a 2,2-dimethylbutyl carbenium ion on the surface they would propagate chain processes, forming the observed 2,2-dimethylbutane by abstracting a hydride from a feed molecule, but they could also desorb to form 2,2-dimethylbutenes. It is the lack of the latter that convinces us that the 2,2 dimethylbutane is formed by a circuitous route.

(*iii*) *Formation of coke and aromatic products.* One more reaction that must be taken into account is the formation of coke, which can be written as the overall process

$$C_jH^+_{2j+1}B^- + C_mH^+_{2m+1}B^- \rightarrow C_jH^+_{2j-1}B^- + C_mH_{2m+2} + H^+B^-, \quad [9]$$

where the $C_jH^+_{2j-1}$ is an olefin ion. Such a species can eliminate saturated molecules and end up as coke or may cyclize and desorb.

As we see in Fig. 4, our product distribution contains secondary aromatic products. The formation of aromatic products must involve the cyclization of larger carbenium ions. Figure 4 shows that the formation of aromatics and other secondary products increases with increasing conversion. We believe that this is so because the higher the conversion of 2,3-dimethylbutane is, the higher the concentration of olefinic products will be. These in turn readily participate in addition reactions with carbenium ions to form larger carbenium ions. Such ions can crack, form nondesorbable residues (coke), or cyclize and release cyclic products, depending on the relative rates of these parallel processes.

(iv) Some observations on the reaction probabilities. Close inspection of Table 4, where the individual reaction paths are presented, together with Table 2, where the experimental initial weight selectivities are reported, makes it possible to make a number of interesting observations regarding the mechanism of this reaction, before we undertake any mathematical manipulation of the data.

The preponderance of C_6 products is obvious from Table 2; they constitute about 85% of the mass of the products on both catalysts. A straightforward translation of these numbers to molar selectivities, as shown in Table 2, shows that some 75% of the molecules produced are C_6 isomers of 2,3-dimethylbutane. This means that process 12 in Table 4 is the dominant process for this molecule. It forms its own reactants (parent carbenium ions) which then isomerize on the surface, only to be displaced by a successive hydride transfer from the feed.

The dominance of this reaction means that there is a large population of C_6 carbenium ions on the surface. Some of this population desorbs, producing the C_6 olefins. Some will undergo β-scission, producing propylene and ethylene, thus explaining the presence of ethylene as a primary product. Most seem to isomerize in steps involving methyl shifts.

The molecules which isomerize will first produce the 2-methylpentyl ion whose saturation by hydride transfer produces 2-methylpentane as the principal product of the reaction. From Table 2 we clearly see that 2,3-dimethylbutane readily rearranges to the more stable 2-methylpentyl form. It is also clear that the rearrangement of 2-methyl to 3-methylpentane is easy, probably because the tertiary carbon in the centre is more stable than in the β position of the chain. This yields 3-methylpentane as the second most plentiful product. Rearrangement of the 2-methylpentyl ion to the linear configuration is clearly difficult and as a result the formation of *n*-hexane is slow, yielding ten times less *n*-hexane than 3-methylpentane.

The last C_6 isomer, 2,2-dimethylbutane, cannot arise by this kind of isomerization without postulating a cyclopropyl ion intermediate. We will not invoke such a postulate since there are no 2,2-dimethylbutenes in the product. Moreover, it would require the formation of 2,2-dimethylbutane in the cracking of 3-methylpentane, where this product is not found. We believe that 2,2-dimethylbutane is formed from isopentyl ions, which are formed from feed molecules by process 2 during initiation and by disproportionation of the feed with propyl ions by process 7. These isopentyl ions abstract a negatively charged methyl group from a feed molecule to form this unexpected product by process 11. Either stearic constraints on the transition state or energy considerations make this an unlikely reaction, and as a result the selectivity for 2,2-dimethylbutane is low.

All the other significant products come from the reactions of propyl ions. The pentyl ions are mostly the result of the transfer of a negatively charged methyl group to a surface propyl ion to release butanes and form a pentyl ion. The pentanes are then formed by the hydride-extraction reactions of pentyl ions.

The importance of the propyl ions is due to the fact that propyl ions are the second most common ions on the surface since they are formed by the preferred form of protolysis of the feed (process 3) and the preferred form of β-cracking of the most plentiful ion on the surface, the parent C_6 ion (process 15). This abundance of propyl ions is also responsible for most of the remaining significant products: propylene (process 15 and desorption of propyl ions), propane (process 3 and 6), and iosbutane (process 7). To put this kind of consideration on a quantitative basis we resort to matrix algebra (23).

(v) Overall reaction rate. A kinetic model suitable for this system has been proposed previously (27). This model accounts for monomolecular and bimolecular processes, both of which are active in 2,3-dimethylbutane cracking, as shown by the initial selectivity data. It assumes that the same sites catalyze both mechanisms, and that the surface reaction is rate controlling. Solution of the model equations yields the rate equation

$$\frac{dX}{d\tau} = \frac{\left[A_1\left[\frac{(1-X)}{(1+\varepsilon X)}\right] + A_2\left[\frac{(1-X)}{(1+\varepsilon X)}\right]^2\right][1+Gt]^{-N}}{1 + B\left[\frac{(1-X)}{(1+\varepsilon X)}\right]}, \quad (10)$$

where X is the instantaneous fractional conversion of re-

TABLE 4

Reaction Pathway Probabilities of 2,3-Dimethylbutane Cracking over USHY and USHY–AHF at 400°C

Entry No.	Reaction		Pathway	RPP USHY	Values USHY–AHF
1	$C_6H_{14} + H^+B^-$		$\xrightarrow{X_{00}} H_2 + C_6H_{13}^+B^-$	0.005	0.002
2			$\xrightarrow{X_{01}} CH_4 + C_5H_{11}^+B^-$	0.021	0.020
3			$\xrightarrow{X_{03}} C_3H_8 + C_3H_7^+E$	0.012	0.013
	Total initiation		Processes	0.018	0.035
4	$C_6H_{14} + C_2H_5^+B^-$		$\xrightarrow{X_{21}} C_2H_6 + C_6H_{13}^+B^-$	[a]	[a]
5			$\xrightarrow{X_{23}} C_5H_{12} + C_3H_7^+B^-$	0.054	0.055
6	$C_6H_{14} + C_3H_7^+B^-$		$\xrightarrow{X_{30}} C_3H_8 + C_6H_{13}^+B^-$	0.025	0.026
7			$\xrightarrow{X_{31}} C_4H_{10} + C_5H_{11}^+B^-$	[a]	[a]
8	$C_6H_{14} + C_4H_9^+B^-$		$\xrightarrow{X_{40}} C_4H_{10} + C_6H_{13}^+B^-$	0.043	0.055
9			$\xrightarrow{X_{41}} C_5H_{12} + C_5H_{11}^+B^-$	[a]	[a]
10	$C_6H_{14} + C_5H_{11}^+B^-$		$\xrightarrow{X_{50}} C_5H_{12} + C_6H_{13}^+B^-$	0.011	0.009
11			$\xrightarrow{X_{51}}$ iso-$C_6H_{14} + C_5H_{11}^+B^-$	0.004	0.004
12	C_6H_{14} + iso-$C_6H_{13}^+B^-$		$\xrightarrow{X_{60}}$ iso-$C_6H_{14} + C_6H_{13}^+B^-$	0.817	0.806
	Total propagation		Processes	0.954	0.955
13	C_6H_{14}		$\xrightarrow{X_{kc}}$ Coke	0.007	0.009
	Initiation + propagation + coking	=	Total conversion reactions	1.0	1.0
14	$C_6H_{13}^+B^-$	or	$\xrightarrow{X_{b62}} C_2H_4 + C_4H_9^+B^-$	0.051	0.060
			$\xrightarrow{X_{b64}} C_4H_8 + C_2H_5^+B^-$		
15	$C_6H_{13}^+B^-$		$\xrightarrow{X_{b63}} C_3H_6 + C_3H_7^+B^-$	[a]	[a]
	Reaction chain length[b]			26.3	28.6

[a] <0.0005.

[b] Calculated by using the method presented in Ref. (22).

actant, τ is the space time, G is the deactivation rate constant, N is the decay exponent, and ε is the volume expansion coefficient.

For the simple case when equilibrium between product olefins and their carbenium ions exists, the constants A_1, A_2, and B are defined by the expressions

$$A_1 = \frac{(\sum k_{Mi})\, K_A + [\sum_i (\sum_j k_{Cj})_i\, K_i\, \mathcal{F}_i] C_{A_0}}{1 + \sum K_i \mathcal{F}_i C_{A_0}} [S]_0 \qquad [11]$$

$$A_2 = \frac{-[\sum_i (\sum_j k_{Cj}) K_i\, \mathcal{F}_i] C_{A_0}}{1 + \sum K_i \mathcal{F}_i C_{A_0}} [S]_0 \qquad [12]$$

$$B = \frac{[K_A - (\sum_i K_i \mathcal{F}_i)] C_{A_0}}{1 + \sum_i K_i \mathcal{F}_i C_{A_0}}, \qquad [13]$$

where

k_{Mi}	is the rate constant of a feed molecule undergoing the ith mode of monomolecular protolysis,
k_{Cj}	is the rate constant of a carbenium ion $C_jH_{2j+1}^+$ and a feed molecule undergoing the jth mode of bimolecular chain reaction,

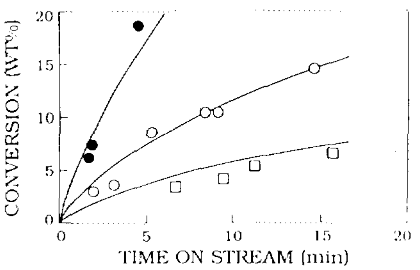

FIG. 5. Theoretical curves and experimental points for the conversion of 2,3-dimethylbutane on USHY at 400°C. Catalyst-to-reactant ratios: (□) 0.0048, (○) 0.0096, and (●) 0.028.

K_A is the adsorption constant of a feed molecule,
K_i is the adsorption constant of the ith product,
C_{A_0} is the initial concentration of reactant,
$[S]_0$ is the initial concentration of active sites, and
$\mathcal{F}_i$ is the molar selectivity of the ith product.

INTERPRETATION OF THE RESULTS

The Kinetics

Experimental average conversions for reactions of 2,3-dimethylbutane on USHY and USHY–AHF at 400°C have been fitted using Eq. [10] as shown in Figs. 5 and 6. Optimum values of the parameters A_1, A_2, B, and G were determined using the sum of squares of residuals as a criterion of fit and are given in Table 3. The value of the decay exponent N was found to be close to one and therefore its value was fixed at 1.0 (24) for both catalysts.

From Table 3 it can be seen that the two values of A_1 are similar, indicating that the total activity via the monomolecular and bimolecular processes varies only slightly due to treatment of USHY with $(NH_4)_2SiF_6$.

The A_2 parameter is necessary in both cases, indicating that the contribution of the chain mechanism is important on both catalysts. The value of A_2 is a larger absolute number for USHY–AHF than for USHY. We do not attach any major significance to this difference, in view of the strong correlation between the A_1 and A_2 parameters in the kinetic rate expression.

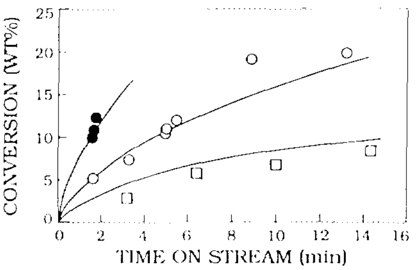

FIG. 6. Theoretical curves and experimental points for the conversion of 2,3-dimethylbutane on USHY–AHF at 400°C. Catalyst-to-reactant ratios: (□) 0.0051, (○) 0101, and (●) 0.026.

The parameter B reflects the relative values of the adsorption constants of reactant and products (27). On both catalysts its value indicates that there is strong preferential adsorption of the product species. The absolute value of this parameter is found to be larger for USHY–AHF than for USHY, suggesting that product species are more strongly adsorbed on USHY–AHF.

Examination of Eq. [13] reveals that the large negative values for B require that both

$$\sum K_i \mathcal{F}_i C_{A_0} \gg 1$$

and [14]

$$\sum K_i \mathcal{F}_i \gg K_A.$$

Using Eq. [14], Eq. [13] reduces to

$$B = \frac{K_A}{\sum K_i \mathcal{F}_i} - 1 \qquad [15]$$

and

$$B + 1 = \frac{K_A}{\sum K_i \mathcal{F}_i} = \frac{K_A}{\overline{K}_p \sum \mathcal{F}_i}, \qquad [16]$$

where $\overline{K}_p = \sum K_i \mathcal{F}_i / \sum \mathcal{F}_i$ is the weighted average adsorption constant for product species. $\sum \mathcal{F}_i$ can be calculated from the sum of the molar selectivities of initial products and is given in Table 2. Rearranging Eq. [16] we get

$$\frac{K_A}{\overline{K}_p} = (B + 1) \sum \mathcal{F}_i. \qquad [17]$$

From Eq. [17] values representative of the ratio of the adsorption constants have been calculated and are listed in Table 5. There it can be seen that the value of $K_A/\overline{K}_p$ for USHY is larger than that for USHY–AHF. The result confirms that the surface of USHY–AHF adsorbs products better than that of USHY. This agrees with the

TABLE 5

Values of the Ratios of Reactant to Product Adsorption Equilibrium Constants, Chain and Monomolecular Reaction Rate Constants for Cracking of 2,3-Dimethylbutane on USHY and USHY-AHF at 400°C

Kinetic parameters	USHY	USHY-AHF
(1) $\frac{K_A}{K_p}$	0.2208	0.1016
$A_1 + A_2$ (min^{-1})	0.5021	0.4241
$B + 1$	0.193	0.088
$\frac{A_1 + A_2}{B + 1}$ (min^{-1})	2.602	4.819

results of Sawa *et al.* (15), who found that dealumination with HCl increased the amount of hydrocarbons adsorbed on the catalyst. This difference does not seem to have any influence on the selectivity of the catalyst.

Information about the initial rate of reaction can be extracted from the results presented in Table 3 by using Eq. [10] under the condition of $\tau = 0$, $X = 0$, that is,

$$\left(\frac{dX}{d\tau}\right)_{\tau \to 0} = \frac{A_1 + A_2}{1 + B}. \qquad [18]$$

Using Eq. [18], we calculate the values of the initiation rate of reaction for the two catalysts listed in Table 5. We find there that the extracted catalyst is almost twice as active in carrying out initiation reactions as USHY. Clearly any increased activity in the protolysis reactions is matched by an increase in the rate of chain propagation so that the initial selectivity stays the same on the two catalysts. This strongly suggests that the removal of EFAl simply makes more sites available for reaction without changing the distribution or acidity of the available sites.

As can be seen in Table 3, there is an increase in the deactivation rate constant G on treatment of USHY with $(NH_4)_2SiF_6$. This agrees with the interpretation that USHY-AHF has more product adsorbed on the surface. The adsorbed product is present in the form of carbenium ions which are the source of coke and deactivation via bimolecular processes we will describe elsewhere.

On the basis of the literature, and considering the results reported here, the observed increase in activity, together with no charge in the initial selectivity, leads us to propose that the conversion of 2,3-dimethylbutane proceeds mainly, probably totally, on the framework Brønsted sites measured here as FAl. The reaction starts off on the pristine Brønsted sites of the framework via protolytic cracking of the feed molecule and proceeds to establish a stable chain mechanism in both cases. The removal of EFAl with $(NH_4)_2SiF_6$ seems to promote both types of conversion processes to the same extent. If the removal of the EFAl were to lead to an increase in the acid strength of the remaining sites, as has been suggested (26), one might expect an increase in the lifetime of carbenium ions on the catalyst surface or some other phenomenon which would change the relative participation of the monomolecular (initiation) and bimolecular (propagation) reactions (12).

Reaction Path Probability (RPP)

The reactions described in the preceding section constitute a chain reaction mechanism consisting of intiation (Eqs. [1] and [2]), propagation (Eqs. [5], [6], and [8]), and termination (Eqs. [7] and [9]). A full set of the pertinent elementary reactions for 2,3-dimethylbutane cracking on USHY and USHY-AHF is presented in Table 4. The RPPs of all individual reaction pathways for our systems have been calculated using the established methodology (23). The results presented in Table 5 show that the sums of the RPP values for bimolecular chain processes are about 0.95 on both USHY and USHY-AHF. The differences are within experimental error in our work and the results therefore show that the two catalysts follow the same mechanism of cracking.

The absence of significant differences in the product distributions obtained on USHY and USHY-AHF may at first appear to arise from the fact that bimolecular reactions, leading to the formation of isomeric products, are dominant in this molecule. This is not so. Since the isomeric products of bimolecular reactions make up about 80% of all the products, any enhancement of monomolecular cracking reactions should be easy to spot in such a system. An increase in bimolecular reactions would also show up clearly as a significant decrease in monomolecular reactions.

There are several reasons that could be put forward to explain the differences in opinion as to the participation of EFAl in catalysis. These include the use of different steaming and calcination methods, different zeolite preparation methods, the extent of dealumination, and the properties of the feed used. Corma *et al.* (21), for example, have observed that the higher the steaming temperature, the more difficult it becomes to extract EFAl using $(NH_4)_2SiF_6$, indicating that there may be different forms of EFAl. They expressed the opinion that higher steaming temperatures produce more highly polymerized EFAl which is more difficult to extract. Others (16) have reported that, depending on the level of extraction, one can obtain an increase or decrease in catalyst activity. Finally, it should be pointed out that treatment of steam-stabilized catalysts with $(NH_4)_2SiF_6$ removes most but not all EFAl.

All the same, in at least one well-characterized system, the one described here, the effect of dealumination is small.

CONCLUSIONS

Our selectivity data show that bimolecular reactions involving hydride ion transfer and disproportionation are the dominant reaction modes for the cracking of 2,3-dimethylbutane on both USHY catalysts. No significant change in the product distribution was observed upon removal of extraframework aluminum from the steamed catalyst.

The data show that treatment of steam-stabilized HY with $(NH_4)_2SiF_6$ results in a small gain in activity. We also find that olefinic products are more strongly adsorbed than 2,3-dimethylbutane on both catalysts but moreso on the catalyst containing no extraframework aluminum. A slight increase in the rate of catalyst decay was also observed on the catalyst free of extraframework aluminum.

Detailed analysis of individual reaction path probabilities indicates that extraframework aluminum plays no significant role in the cracking of 2,3-dimethylbutane at 400°C. We believe that the EFAl produced by steaming simply blocks pores or covers individual sites indiscriminately. Perhaps the effects observed by other workers can be explained in terms of site density effects or in terms of stearic constraints. In the case of catalyst formulations containing an active matrix or other active components, changes in overall selectivity may be the result of an increased activity on the extracted zeolite component.

ACKNOWLEDGMENT

The authors are grateful to Dr. W. A. Groten for assistance with ^{27}Al MAS NMR measurements.

REFERENCES

1. Mirados, C., and Barthomeuf, D., *J. Chem. Soc. Chem. Commun.*, 39 (1981).
2. Haag, W. O., *in* "Proceedings of 6th International Zeolite Symposium, Tokyo" (D. H. Olson and A. Bisio, Eds.), p. 466. Butterworths, London, 1984.
3. Ward, J. W., and Carlson, T. L., U.S. Patent 4,517,073, May 14, 1985.
4. DeCanio, S. J., John, J. R., Fritz, P. O., and Lunsford, J. H., *J. Catal.* **101,** 132 (1986).
5. Beyerlein, R. A., McVicker, G. B., Yacullo, L. N., and Ziemiak, J. J., *J. Phys. Chem.* **92,** 1967 (1988).
6. Brunner, E., Ernst, H., Feude, D., Frohlich, T., Hunger, M., and Pfeifer, H., *J. Catal.* **127,** 34 (1991).
7. de Kroes, B., Groenenbroom, C. J., and O'Connor, P., Ketjen Catalyst Symposium, Paper F-1 (1986).
8. Nock, A., and Rudham, R., *Zeolites* **7,** 481 (1987).
9. Pellet, R. J., Blackwell, C. S., and Rabo, J. A., *J. Catal.* **114,** 71 (1988).
10. Macedo, A., Ph.D. ENSPM, Rueil Malmaison, France, 1988.
11. Richter, M., Fiebig, W., Jerschkewitz, H. G., Lischke, G., and Ohlmann, G., *Zeolites* **9,** 238 (1989).
12. Engelhardt, J., and Hall, W. K., *J. Catal.* **125,** 472 (1990).
13. Machado, F., Magnoux, P., and Guisnet, M., *in* "Proceeding 5th International Symposium Evanston, IL" (C. H. Bartholomew and J. B. Butt, Eds.), p. 807 Elsevier, New York 1991.
14. Creighton, J. E., Edwards, G. C., Rajagopalan, K., Peters, A. W., and Young, G. W., *Am. Chem. Soc., Div. Pet. Chem.* **32**(3), 617 (1987); *in* "Fluid Catalytic Cracking: Role in Modern Refining" (M. C. Ocelli, Ed.), p. 101. ACS Symposium Series, Vol. 375, American Chemical Society, Washington, DC, 1988.
15. Sawa, M., Niwaand, M., and Murakami, Y., *Appl. Catal.* **53,** 169 (1989).
16. Jacquinot, E., Raatz, F., Macedo, A., and Maralay, C., *in* "Zeolites and Catalysts, Sorbents and Detergent Builders," (H. G. Karge and S. Weitkamp, Eds.), p. 377. Elsevier, Amsterdam, 1989.
17. Chauvin, B., Massiani, P., Dutartre, R., Figueras, F., Fajula, F., and Courieres, T. D., *Zeolites* **10,** 174 (1990).
18. Breck, D. W., and Skeels, G. W., *in* "Proceeding, 6th International Zeolite Conference Reno, 1983" (D. Olson and A. Bisio, Eds.) p. 87). Butterworths, London, 1984.
19. Chauvin, B., Boulet, M., Massian, P., Fajula, F., Figueras, F., and Courieres, T. D., *J. Catal.* **126,** 532 (1990).
20. Kerr, G. T., *Zeolites* **9,** 350 (1989).
21. Corma, A., Fornes, V., and Rey, F., *Appl. Catal.* **59,** 267 (1990).
22. Zhao, Y. X., Bamwenda, G. R., and Wojciechowski, B. W., *J. Catal.* **142,** 465 (1993).
23. Zhao, Y. X., and Wojciechowski, B. W., *J. Catal.* **142** 499 (1993).
24. Ko, A. N., and Wojciechowski, B. W., *Prog. React. Kinet.* **12**(4), 201 (1983).
25. Haag, W. O., and Dessau, R. M., *in* "Proceedings of 8th International Congress on Catalysis, Berlin, 1984, Vol. 2, p. 305. Dechema, Frankfurt-am-Main, 1984.
26. Beaumont, R., and Barthomeut, D., *J. Catal.* **26,** 218 (1972).
27. Groten, W. A., and Wojciechowski, B. W., *J. Catal.* **140** 262 (1993).